CrossMark

Effect of Metal Doped Zinc Oxide Nanorods on Photoelectrical Characteristics of ZnO/Polyaniline Heterojunction

Jyoti M. Ghushe[1] · Sushama M. Giripunje[2] · Subhash B. Kondawar[3]

Abstract The *n*-type vertically aligned metal doped ZnO nanorods (NRs) and *p*-type proton acid doped polyaniline (PANI) inorganic/organic heterojunction diodes have been fabricated. Aluminium (Al) and iron (Fe) doped ZnO NRs were grown on seed ZnO layer on fluorine doped tin oxide coated glass substrates by high temperature chemical bath deposition method. The elemental analysis using EDAX confirm doping of Al and Fe in ZnO. The morphology of doped ZnO nanorods and ZnO/PANI heterojunction exhibit well defined uniform nanorod arrays and interface between nanorods and polyaniline matrix respectively. The dark current–voltage curves confirmed the rectifying diode like behaviors of the heterojunctions, whereas under illumination, the junction revealed good sensitivity to UV and visible range with increased current densities. The highest ideality factor and lowest barrier height was found for FeZnO/PANI heterojunction under dark and under light compared to that of ZnO/PANI, AlZnO/PANI. This research is innovative with respect to low cost synthesis of efficient and sensitive hybrid *p–n* junction diodes and possibly serves as the building blocks for future optoelectronic applications.

Keywords Metal doped ZnO nanorods · Polyaniline · Ideality factor · Barrier height · Hybrid *p–n* junction

✉ Sushama M. Giripunje
smgiripunje@phy.vnit.ac.in

1 Department of Applied Physics, Priyadarshini College of Engineering, Nagpur 440018, India

2 Department of Applied Physics, Visvesvaraya National Institute of Technology, Nagpur 440010, India

3 Department of Physics, Rashtrasant Tukadoji Maharaj Nagpur University, Nagpur 440033, India

1 Introduction

Hybrid inorganic/organic heterojunction devices have received much attention as promising junctions for widespread applications. There are reports available on the use of these heterojunctions as gas sensors, light emitting diodes, photo detectors and solar cells [1–4]. Transparent conducting oxide (TCO) serves as the inorganic semiconductor in these heterojunctions. Zinc oxide (ZnO) is one of such famous transparent conducting oxides [5]. ZnO, especially in its nanostructured form, has been considered to be attractive because of the wide band gap (3.4 eV) and high exciton binding energy (60 meV). However, it is difficult to fabricate ZnO with stable *p*-type conductivity because of its intrinsically *n*-type nature. The *n*-type behavior is typically because of the interstitial defects and oxygen vacancies in ZnO wurtzite structure. The difficulty in doping ZnO to *p*-type impurity has led the researchers to prepare the heterojunctions with other *p*-type semiconductors for its use in various electronic devices [6]. The quality of *p–n* heterojunction is mainly limited by the lattice mismatch. This difficulty gets resolved by using ZnO nanostructures. The nanostructures of ZnO possess self organized growth property which enables easy growth of p type material over n type material thus producing heterojunctions of quality devices by using external *p*-type materials [7]. In addition, ZnO nanorods provide large surface area which is useful for the heterojunction formation. ZnO/organic hybrid structure has found importance in solar cell, photodiodes, photovoltaic and photochemical applications. The electrical conductivity of ZnO can be increased by adding a small amount of impurity(doping) e.g. alkali metals like B, Li [8] or metals like Al [9], Fe [10, 11], Cu [12], Ni [13], Co [14] and Ga [15, 16] etc. There are reports available for higher values of conductivities

with unchanged crystal structure of zinc oxide thin films upon doping with Al and Fe [17, 18].

The *p*-type conducting polymer polyaniline (PANI) has many advantages including easy fabrication, flexibility, and tunable carrier densities. It is environmentally stable and its electrical properties can be tuned to its various oxidation states from emeraldine base to salt form [19]. Kovtyukhova et al. [20] was the first to study nanostructured composite of ZnO/PANI with rectifying property of the junction. Mridha and Basak [21] prepared a single layer ZnO/PANI hybrid structure by using sol gel method. They reported I–V characteristics of the junction with rectifying behavior. Sharma et al. [22] studied ZnO/polyaniline heterojunction and reported that the heterojunction shows good rectifying behavior with ideality factor of 3.1 and barrier height about 0.68 eV. They reported that the higher value of ideality factor may be attributed to many current paths available due to ZnO nanostructures. Tang et al. [23], reported fabrication and characterization of *p–n* heterojunction on ordered ZnO nanowires/polyaniline microrods double array. Liu et al. [2], reported flexible blue light emitting diode based on ZnO nanowire/polyaniline heterojunctions. Sharma and Khare [24], reported effect of UV exposure on rectifying behavior of ZnO/PANI heterojunction. They reported that I–V characteristics of ZnO/PANI showed diode like behavior with ideality factor of 1.54 and barrier height equal to 1.35 eV. Upon UV exposure, diode showed rise in ideality factor equal to 7.94 and fall in barrier height to 0.92 eV. Yakuphanoglu et al. [25], reported the electrical and photovoltaic properties of the nanostructure ZnO/*p*-Si diode with the ideality factor and barrier height of 3.18 and 0.78 eV, respectively. Ameen et al. [26] reported electrophoretically deposited polyaniline/ZnO nanoparticles for *p–n* heterostructure diodes.

Thus, *n*-type ZnO/*p*-type polyaniline heterostructures have been fabricated and studied. There are also a variety of papers on synthesis and characterization of metal doped ZnO NRs. However, metal doped ZnO/polyaniline heterojunctions have not been systematically studied. We synthesized metal doped (Al and Fe) ZnO NRs using simple solution chemistry methods (SILAR and HTCBD). Their morphology studies were done using SEM and EDAX. The AlZnO/PANI, FeZnO/PANI and ZnO/PANI heterojunctions were fabricated. The I–V characteristics under illumination were studied using solar simulator. A detailed study of such heterojunctions and estimation of the diode parameters like ideality factor and barrier heights was carried out. The effect of doping in ZnO on the I–V characteristics of heterojunctions in dark and light conditions is highlighted. The study is new, innovative and useful for applications in various optoelectronic devices.

2 Experimental

2.1 Materials

The chemicals like ammonium peroxy disulphate, HCl, aniline were purchased from Merck. The chemicals were of analytical grades and the aniline was distilled prior to use. Zinc acetate and Hexamethylene tetramine (HMTA) of AR grade were purchased from Qualigens. FTO slides were thoroughly washed using soap solution, ultrasonicated for 15 min in isopropanol, then for 15 min in soap solution. Finally, the slides were cleaned with soap solution till a uniform water film is seen on FTO surface. The sheet resistance of the FTO slide was measured to be 14–15 Ω.

2.2 Fabrication of Zinc Oxide/Polyaniline Heterojunction Diodes

Zinc oxide seeded/compact layer was deposited using aqueous ammonium zincate complex as cationic precursor and double distilled hot water as anionic precursor by a successive ionic layer adsorption reaction (SILAR) method. The aqueous ammonium zincate complex bath was prepared by adding NH_3 solution to 0.02 M zinc acetate dehydrate $Zn(CH_3COO)_2 \cdot 2H_2O$. The pH of the solution was maintained to 10–11. Seeded ZnO layer was deposited on cleaned FTO glass substrate. The number of deposition cycles was optimized to get the seed layer of desired thickness. After the deposition, the films were dried in hot air oven at 200 °C for 1 h. Compact/Seed layer is necessary as a blocking layer to prevent direct contact between hole conductor and the conducting glass. To avoid short circuit, use of seed layer prior to porous ZnO thin film deposited by HTCBD is essential. These seeded ZnO layers (films) were further used for fabrication of ZnO nanorods by high temperature chemical bath deposition (HTCBD). In this method, aqueous bath was prepared using equimolar concentrations of zinc acetate and HMTA (0.025 M) and ammonia solution (pH 8–9). The zincate complex solution was kept in hot water bath (90–95 °C), and FTO slide was kept vertically immersed in the solution. Ammonia solution was added for slow nucleation and growth of zinc oxide nanorods onto the FTO slides. The film was taken after about 1 h., washed with double distilled water and annealed in hot air oven at 200 °C for 1 h. Al and Fe doped ZnO nanorods were grown using $AlCl_3$ and $FeCl_3$ with 3 mol% (Al/Zn and Fe/Zn) in the zincate bath and similar procedure followed. According to normal doping rules, substitution of Al^{3+} or Fe^{+3} at the Zn^{2+} sites creates one extra free carrier in the process and occupies Zn^{2+} sites up to the solubility. Therefore, increase of carrier concentration up to the solubility limit is logical but beyond

solubility limit a new phase of Al_2O_3 or Fe_2O_3 arises and therefore substitution of Al or Fe is no longer effective as before. Also, after a certain level of doping, the extra Al or Fe atoms may occupy the interstitial positions and form corresponding oxides leading to distortion of the crystal structure which gives rise to the greater electron scattering, i.e. higher resistance [13, 21]. On the surface of ZnO and Al and Fe doped ZnO nanorods, thin layer of polyaniline was deposited by spin coating at a rate of 3000 rpm. The layout of fabricated nanostuctured heterojunction of polyaniline and ZnO is shown in Fig. 1.

2.3 Characterizations

The surface morphology of ZnO, Al doped ZnO and Fe doped ZnO thin films and ZnO/polyaniline was studied by JEOL 6380A scanning electron microscope. The current–voltage measurements of were performed using Keithley's 2611B current meter for all the thin film heterojunctions. The solar simulator AM 1.5G was used to illuminate the junction and the illumination area was approximately 1 cm^2. The current values with and without illumination were compared.

3 Results and Discussion

3.1 Morphology

The SEM images of ZnO seed layer and ZnO nanorods are shown in Fig. 2a, b respectively. Seeds of ZnO are clearly seen in the figures whereas, the average length of ZnO nanorods and diameter was found to be 1–2 μm and 100–200 nm respectively. SEM images of Al doped ZnO nanorods and Fe doped ZnO nanorods at 3.00 μm and 500 nm resolution are shown in Figs. 3 and 4 respectively. The average diameter of Fe doped ZnO nanorods was found to be smaller than that of Al doped ZnO nanorods and undoped ZnO nanorods. The enhanced surface area of Fe doped ZnO nanorods is the key factor to show the improvement in photoelectrical property of Fe doped ZnO/PANI heterojunction compared to that of undoped and Al doped ZnO/PANI heterojunction. EDAX images of Al

Fig. 1 Layout of polyaniline/ZnO heterojunction

doped and Fe doped ZnO nanorods clearly shows the presence of Al/Fe, Zn, O as shown in Fig. 5. Polyaniline is uniformly deposited over the surface of ZnO nanorods by using spin coating as shown in the cross sectional view of ZnO/polyaniline heterojunction (Fig. 6).

3.2 I–V Characteristics in Dark and Illuminated Conditions

I–V characteristics for pure ZnO and polyaniline thin films are shown in Fig. 7. The studies on the I–V characterization of the fabricated ZnO/PANI, AlZnO/PANI and FeZnO/PANI heterojunctions under dark conditions revealed a good p–n junction diode like rectifying behavior (Fig. 8). The DC rectification ratios (defined as the forward current divided by the reverse current at a bias) are found to be about 10, 55, 12 at ±1 V in dark and approximately 4, 7 and 40 at ±1 V in illuminated conditions respectively for each of the diodes. The rectification ratio for FeZnO/PANI was found to be increased in the illuminated conditions. The turn on voltages for ZnO/PANI, AlZnO/PANI and FeZnO/PANI are in the range 0.6–0.7 V and the reverse saturation current values calculated at −1.0 V are 10, 4, and 44 μA respectively. Thus, it is confirmed that a proper p–n junction is formed between undoped and doped ZnO nanorods with polyaniline.

The diode like behavior of metal doped and undoped ZnO/polyaniline heterojunctions were examined using thermionic emission model [27]. According to this model, the junction under forward bias has the I–V relation given by,

$$I = I_s\left[exp\frac{qV}{\eta KT} - 1\right]. \tag{1}$$

where I_s is the saturation current, q is the elementary charge, V is the applied voltage, η is ideality factor, K is Boltzmann constant and T is absolute temperature.

The barrier height was calculated using relation $I_s = AA^*T^2exp\left[\frac{-q\Phi_b}{KT}\right]$ where A is diode area = 1 cm^2, $A^* = 36A\ cm^{-2}\ K^{-2}$ for ZnO ($m_e^* = 0.3m_0$) is Richardson's constant and Φ_b is the barrier height at the diode interface.

The ideality factors η and barrier height Φ_b for ZnO/PANI, AlZnO/PANI and FeZnO/PANI calculated from ln I versus V graph and found to be 1.93, 2.32 and 3.367 and 0.786, 0.781, and 0.670 eV respectively. Sharma et al. [22], reported ideality factor of 3.1 and barrier height of 0.68 eV for ZnO/polyaniline heterojunction. A greater value than 2 for η indicates that the diodes are not ideal ones. Higher values of η can be attributed to the presence of the interfacial thin native oxide layer, series resistance etc. The higher values of ideality factor in all the junctions may be
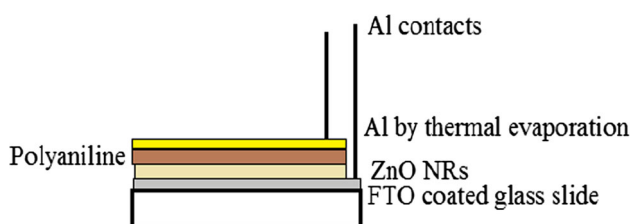
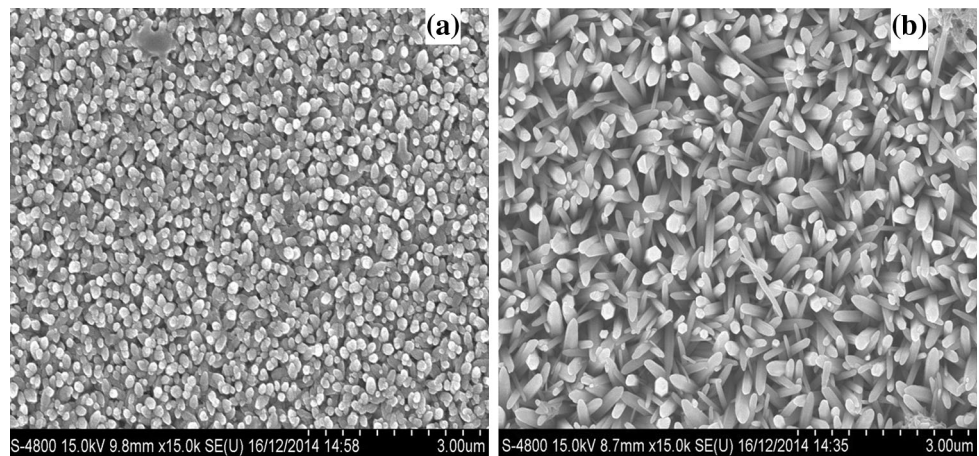**Fig. 2** SEM image of **a** ZnO seed layer and **b** ZnO nanorods

Fig. 3 SEM image of Al doped ZnO nanorods. **a** At 3.00 μm and **b** 500 nm resolution
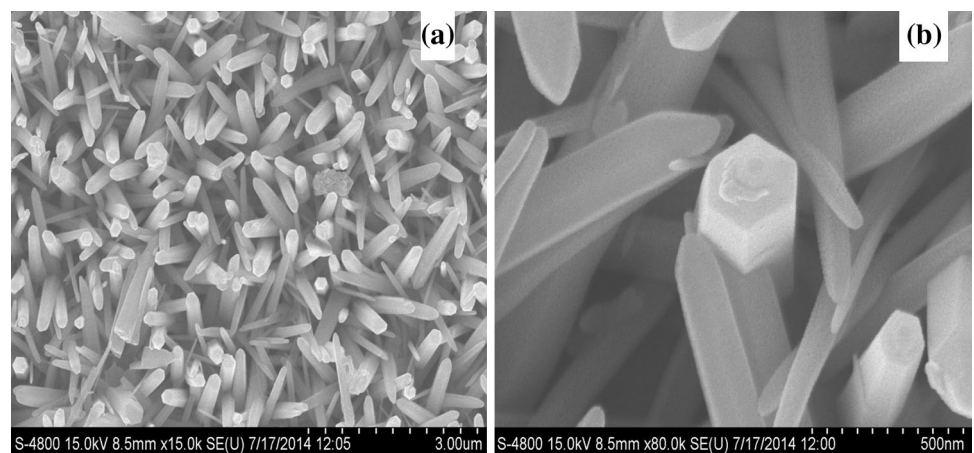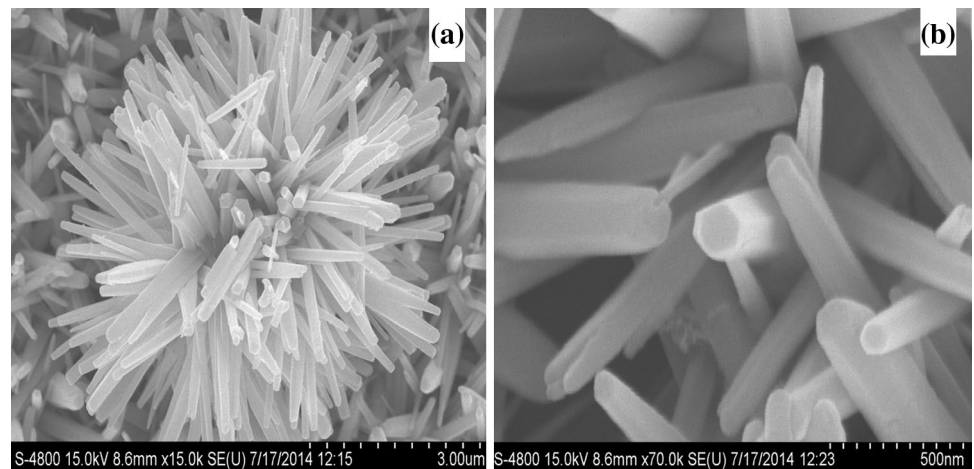

Fig. 4 SEM image of Fe doped ZnO nanorods. **a** At 3.00 μm and **b** 500 nm resolution

attributed to the existence of multiple paths for current due to the presence of defects in the annealed ZnO and doped ZnO thin film. Multistep tunneling at the *p–n* junction would result in an excess current [11, 28–31].

The photo I–V characteristics measured by illuminating all the heterojunctions are shown in Fig. 9. Upon illumination with the light, both the forward and reverse currents were found to be increased as compared to that of under d-

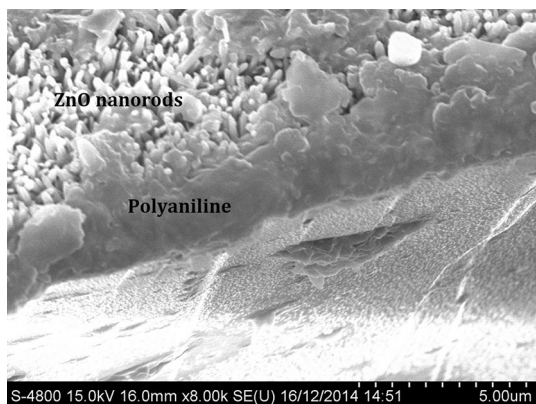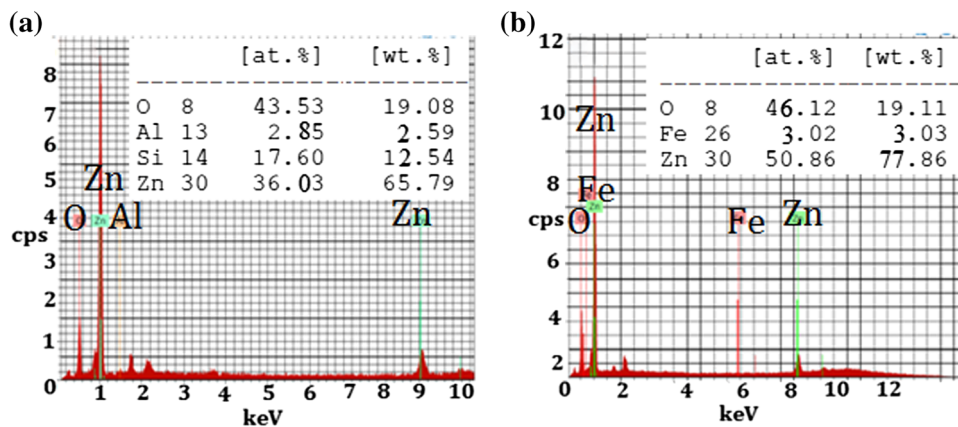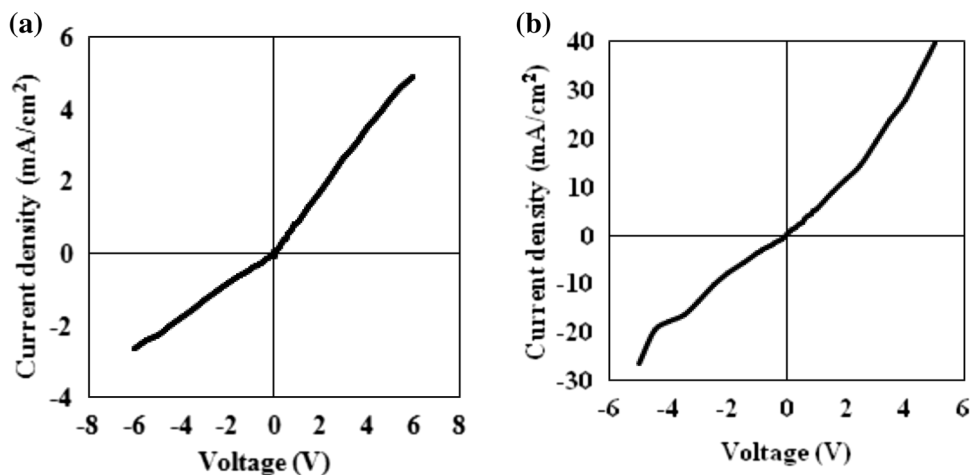**Fig. 5** EDAX images of **a** Al doped and **b** Fe doped ZnO nanorods

Fig. 6 SEM image of ZnO/polyaniline heterojunction cross section

Fig. 8 I–V characteristics of the *a* ZnO/PANI, *b* AlZnO/PANI, and *c* FeZnO/PANI heterojunctions under dark conditions

Fig. 7 I–V characteristics of pure. **a** ZnO thin film and **b** polyaniline thin film

ark conditions. The turn on voltage was found to be reduced in each case, which may be attributed to the reduction of the potential barrier, resulting in current enhancement at a fixed voltage value. The ideality factors for ZnO/PANI, AlZnO/PANI and FeZnO/PANI heterojunctions under illumination were also calculated by similar calculations and the values were found to be 3.015, 2.849 and 6.289 respectively whereas the barrier heights reduced upon illumination to the values 0.640, 0.702, and 0.628 eV respectively. All the results of ideality factor and barrier heights are fairly reproducible. The reverse saturation currents were found to be decreased upon illumination to the values 9, 4.2, and 39.5 µA for ZnO/PANI, AlZnO/PANI and FeZnO/PANI heterojunctions.
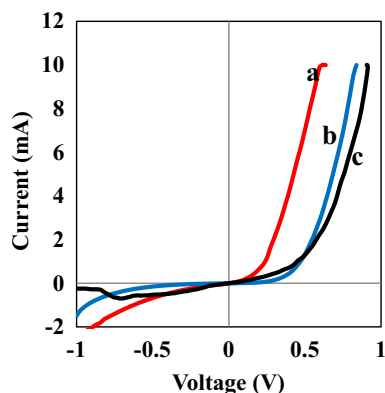
Fig. 9 I–V characteristics of *a* ZnO/PANI, *b* AlZnO/PANI, and *c* FeZnO/PANI heterojunctions under illuminated conditions

4 Conclusion

The hybrid heterojunction diodes with undoped and metal doped vertically aligned *n*-type ZnO NRs and *p*-type polyaniline are successfully fabricated and photoelectrical performances are investigated. All the heterojunctions demonstrate asymmetric diode like rectifying behaviors. The highest ideality factor and lowest barrier height was observed for FeZnO/PANI junction. The photoelectrical measurements demonstrate that the heterojunctions based on ZnO NRs has a high selectivity to visible light. The photo response of all as-fabricated heterojunctions indicated increase current in forward and reverse bias and decrease in turn on voltage upon doping. The photo response properties of these heterojunctions are useful in various optoelectronic and photovoltaic applications.

References

1. J. Gong, Y. Li, Z. Hu, Z. Zhou, Y. Deng, J. Phys. Chem. C **144**, 9970 (2010)
2. Y. Liu, X. Wang, Y. Cao, X. Chen, S. Xie, X. Zheng, H. Zeng, J. Nanomater. **2013**, 1 (2013)
3. W.E. Mahmoud, J. Phys. D **42**, 1555502 (2009)
4. S. Almohsin, S. Al-Mutoki, Z. Li, J. Ark. Acad. Sci. **66**, 26 (2012)
5. Y. Liu, Y. Li, H. Zeng, J. Nanomater. **2013**, 1 (2013)
6. L. Felix, E.F. da Silva Jr, E.A. de Vasconcelos, W.M. de Azevedo, J. Korean Phys. Soc. **58**, 1256 (2011)
7. J. Liu, S. Wang, Z. Bian, M. Shah, C. Huang, Appl. Phys. Lett. **94**, 173107 (2009)
8. S. Chawla, K. Jayanti, R. Kotnala, Phys. Rev. B **79**, 125204 (2009)
9. H.M. Zhou et al., Thin Solid Films **515**, 6909 (2007)
10. S.M. Salaken, E. Farzana, J. Podder, J. Semicond. **34**(7), 073003-1–073003-6 (2013)
11. L. Xu, X. Li, J. Cryst. Growth **312**, 851 (2010)
12. S.Y. Pung, C.S. Ong, K. Mohd. Isha, M.H. Othman, Sains Malays. **43**(2), 273 (2014)
13. C. Cheng, G. Xu, H. Zhang, Y. Leu, Mater. Lett. **62**, 1617 (2008)
14. A. Ghosh, N. Karak, T.K. Kundu, AIP Conf. Proc. **177**, 1536 (2013)
15. Y. Kim, B.H. Kong, H. Kouncho, J. Cryst. Growth **330**(1), 17 (2011)
16. S. Young, J. Nanosci. Nanotech. **13**, 1 (2013)
17. J. Chen, J. Wang, R. Zhuo, D. Yan, J. Feng, F. Zhang, P. Yan, Appl. Surf. Sci. **255**, 3959 (2009)
18. C. Guillen, J. Herrero, Vacuum **84**, 924 (2010)
19. J. Stejskal, R. Gilbert, Pure Appl. Chem. **74**(5), 857 (2002)
20. N. Kovtyukhova, A. Gorchinskiy, C. Waraksa, Mater. Sci. Eng. B **69**, 424 (2000)
21. S. Mridha, D. Basak, Appl. Phys. Lett. **92**, 142111–142113 (2008)
22. B. Sharma, B. Banothu, N. Khare, Polyaniline/ZnO heterojunction. AIP Conf. Proc. **713**, 1349 (2011)
23. Q. Tang, L. Lin, X. Zhao, K. Huang, J. Wu, Langmuir **28**(8), 3972 (2012)
24. B. Sharma, N. Khare, Semicond. Sci. Technol. **28**(12), 5022 (2013)
25. F. Yakuphanoglu, Y. Caglar, M. Caglar, S. Ilican, Mater. Sci. Semicond. Proc. **13**(3), 137 (2010)
26. S. Ameen, S. Ansari, M. Song, Y. Kim, H. Shin, Superlatt. Microst. **46**(5), 745 (2009)
27. S. Sze, *Semiconductor Devices*, 2nd edn. (Wiley, New York, 2001)
28. M. Kuik, H. Nicolai, M. Lenes, G. Wetzelaer, M. Lu, P. Blom, Appl. Phys. Lett. **98**, 093301 (2011)
29. T. Kirchartz, B. Pieters, J. Kirkpatrick, U. Rau, J. Nelson, Phys. Rev. B **83**, 115209 (2011)
30. S. Cowan, W. Leong, N. Banerji, G. Dennler, A. Heeger, Adv. Funct. Mater. **21**, 3083 (2011)
31. L. Koster, V. Mihailetchi, R. Ramaker, P. Blom, Appl. Phys. Lett. **86**, 123509 (2005)